

## Kaon-, $\Lambda$ - and $\bar{\Lambda}$ -production in Pb + Pb-collisions at 158 GeV per nucleon

Christian Bormann<sup>†</sup> for the NA49 Collaboration

Institut für Kernphysik, Universität Frankfurt, August-Euler Strasse 6, D-60486 Frankfurt, Germany

T Alber<sup>13</sup>, H Appelshäuser<sup>7</sup>, J Bächler<sup>5</sup>, S J Bailey<sup>16</sup>, L S Barnby<sup>3</sup>,  
 J Bartke<sup>6</sup>, H Białkowska<sup>14</sup>, C O Blyth<sup>3</sup>, R Bock<sup>7</sup>, C Bormann<sup>10</sup>,  
 F P Brady<sup>8</sup>, R Brockmann<sup>7</sup>, N Buncic<sup>5,10</sup>, P Buncic<sup>5,10</sup>, H L Caines<sup>3</sup>,  
 D Cebra<sup>8</sup>, P Chan<sup>16</sup>, G E Cooper<sup>2</sup>, J G Cramer<sup>16,13</sup>, P B Cramer<sup>16</sup>,  
 P Csato<sup>4</sup>, J Dunn<sup>8</sup>, V Eckardt<sup>13</sup>, F Eckhardt<sup>12</sup>, M I Ferguson<sup>5</sup>,  
 H G Fischer<sup>5</sup>, D Flierl<sup>10</sup>, Z Fodor<sup>4</sup>, P Foka<sup>7,10</sup>, P Freund<sup>13</sup>, V Friese<sup>12</sup>,  
 M Fuchs<sup>10</sup>, F Gabler<sup>10</sup>, J Gal<sup>4</sup>, M Gaździcki<sup>10</sup>, E Gładysz<sup>6</sup>,  
 J Grebieszko<sup>15</sup>, J Günther<sup>10</sup>, J W Harris<sup>17</sup>, S Hegyi<sup>4</sup>, T Henkel<sup>12</sup>,  
 L A Hill<sup>3</sup>, I Huang<sup>2,8</sup>, M A Howe<sup>16</sup>, H Hümmeler<sup>10</sup>, G Igo<sup>11</sup>,  
 D Irmscher<sup>2,7,‡</sup>, P Jacobs<sup>2</sup>, P G Jones<sup>3</sup>, K Kadija<sup>18,13</sup>, V I Kolesnikov<sup>9</sup>,  
 M Kowalski<sup>6</sup>, B Lasiuk<sup>11</sup>, P Lévai<sup>4</sup>, A I Malakhov<sup>9</sup>, S Margetis<sup>2,§</sup>,  
 C Markert<sup>7</sup>, G L Melkumov<sup>9</sup>, A Mock<sup>13</sup>, J Molnár<sup>4</sup>, J M Nelson<sup>3</sup>,  
 G Odyniec<sup>2</sup>, G Palla<sup>4</sup>, A D Panagiotou<sup>1</sup>, A Petridis<sup>1</sup>, A Piper<sup>12</sup>,  
 R J Porter<sup>2</sup>, A M Poskanzer<sup>2,||</sup>, S Poziombka<sup>10</sup>, D J Prindle<sup>16</sup>,  
 F Pühlhofer<sup>12</sup>, W Rauch<sup>13</sup>, J G Reid<sup>16</sup>, R Renfordt<sup>10</sup>, W Retyk<sup>15</sup>,  
 H G Ritter<sup>2</sup>, D Röhrich<sup>10</sup>, C Roland<sup>7</sup>, G Roland<sup>10</sup>, H Rudolph<sup>2,10</sup>,  
 A Rybicki<sup>6</sup>, I Sakrejda<sup>2</sup>, A Sandoval<sup>7</sup>, H Sann<sup>7</sup>, A Yu Semenov<sup>9</sup>,  
 E Schäfer<sup>13</sup>, D Schmischke<sup>10</sup>, N Schmitz<sup>13</sup>, S Schönfelder<sup>13</sup>, P Seyboth<sup>13</sup>,  
 J Seyerlein<sup>13</sup>, F Sikler<sup>4</sup>, E Skrzypczak<sup>15</sup>, G T A Squier<sup>3</sup>, R Stock<sup>10</sup>,  
 H Ströbele<sup>10</sup>, I Szentpetery<sup>4</sup>, J Sziklai<sup>4</sup>, M Toy<sup>2,11</sup>, T A Trainor<sup>16</sup>,  
 S Trentalange<sup>11</sup>, T Ullrich<sup>17</sup>, M Vassiliou<sup>1</sup>, G Vesztergombi<sup>4</sup>, D Vranic<sup>7,18</sup>,  
 F Wang<sup>2</sup>, D D Weerasundara<sup>16</sup>, S Wenig<sup>5</sup>, C Whitten<sup>11</sup>, T Wienold<sup>2,‡,¶</sup>,  
 L Wood<sup>8</sup>, T A Yates<sup>3</sup>, J Zimanyi<sup>4</sup>, X -Z Zhu<sup>16</sup>, R Zybent<sup>3</sup>

<sup>1</sup> Department of Physics, University of Athens, Athens, Greece

<sup>2</sup> Lawrence Berkeley National Laboratory, University of California, Berkeley, USA

<sup>3</sup> Birmingham University, Birmingham, UK

<sup>4</sup> KFKI Research Institute for Particle and Nuclear Physics, Budapest, Hungary

<sup>5</sup> CERN, Geneva, Switzerland

<sup>6</sup> Institute of Nuclear Physics, Cracow, Poland

<sup>7</sup> Gesellschaft für Schwerionenforschung (GSI), Darmstadt, Germany

<sup>8</sup> University of California at Davis, Davis, USA

<sup>9</sup> Joint Institute for Nuclear Research, Dubna, Russia

<sup>10</sup> Fachbereich Physik der Universität, Frankfurt, Germany

<sup>†</sup> E-mail address: bormann@ikf.uni-frankfurt.de

<sup>‡</sup> Alexander von Humboldt Foundation (Lynen) Fellow.

<sup>§</sup> Present address: Brookhaven Nation Laboratory, Upton, NY, USA.

<sup>||</sup> Alexander von Humboldt Foundation US Senior Scientist Award Recipient.

<sup>¶</sup> Present address: Physikalisches Institut, Universität Heidelberg, Germany.

<sup>11</sup> University of California at Los Angeles, Los Angeles, CA, USA

<sup>12</sup> Fachbereich Physik der Universität, Marburg, Germany

<sup>13</sup> Max-Planck-Institut für Physik, Munich, Germany

<sup>14</sup> Institute for Nuclear Studies, Warsaw, Poland

<sup>15</sup> Institute for Experimental Physics, University of Warsaw, Warsaw, Poland

<sup>16</sup> Nuclear Physics Laboratory, University of Washington, Seattle, WA, USA

<sup>17</sup> Yale University, New Haven, CT, USA

<sup>18</sup> Rudjer Boskovic Institute, Zagreb, Croatia

Received 1 October 1997

**Abstract.** Preliminary inclusive spectra for  $K^+$ ,  $K^-$ ,  $K_s^0$ ,  $\Lambda$ , and  $\bar{\Lambda}$  are presented which were measured in central Pb + Pb collisions at 158 GeV per nucleon by the NA49 experiment. A comparison with data from lighter collision systems shows a strong change of the shape of the  $\Lambda$  rapidity distribution. The strangeness enhancement observed in S + S compared to p + p and p + A is not further increased in Pb + Pb.

## 1. Introduction

The ultimate goal of studying collisions of ultrarelativistic heavy nuclei is the observation of a quark–gluon plasma (QGP), a state of deconfined quarks and gluons. The hot and dense nuclear matter created over a large volume in central Pb + Pb collisions at 158 GeV per nucleon constitutes the best laboratory environment for such studies. An enhanced production of strange particles has long been proposed as one of the signatures of the quark–gluon plasma formation [1].

## 2. Experimental set-up

The fixed-target experiment NA49 is located at the 158 GeV per nucleon lead beam of the SPS at CERN. In a central Pb + Pb collision about 1600 charged particles are produced of which about 60% are detected by the NA49 detectors. The main detectors of the NA49 experiment (figure 1) are the four large volume time projection chambers (TPC). Two of these three-dimensional tracking detectors, the vertex-TPCs (VTPC), are located in the magnetic field of two superconducting dipole magnets with a total bending power of 9 Tm. The momentum of tracks registered in the VTPCs is determined from the curvature of the particle tracks. The other two TPCs are located behind the vertex magnets. Their length was optimized for a specific energy loss ( $dE/dx$ ) resolution of better than 5%. The set-up is augmented by four highly segmented time-of-flight (TOF) walls.

Two calorimeters further downstream from the TPCs are used for event characterization. The veto-calorimeter measures the forward energy distribution. With an online-cut in this distribution only the 4% most central events are selected from all inelastic Pb+Pb collisions. This corresponds to an impact parameter of about  $b \leq 3.5$  fm.

## 3. Measurement methods for strange particles

Kaons and lambdas can be distinguished into neutral ( $\Lambda$ ,  $\bar{\Lambda}$ ,  $K_s^0$ ) and charged strange particles ( $K^+$ ,  $K^-$ ). Neutral strange particles are identified by their characteristic V-decay topology. The charged kaons are seen in the NA49 detectors and identified by TOF, energy loss, or decays.

The acceptance of the NA49 detectors for kaons and lambdas is shown in table 1.

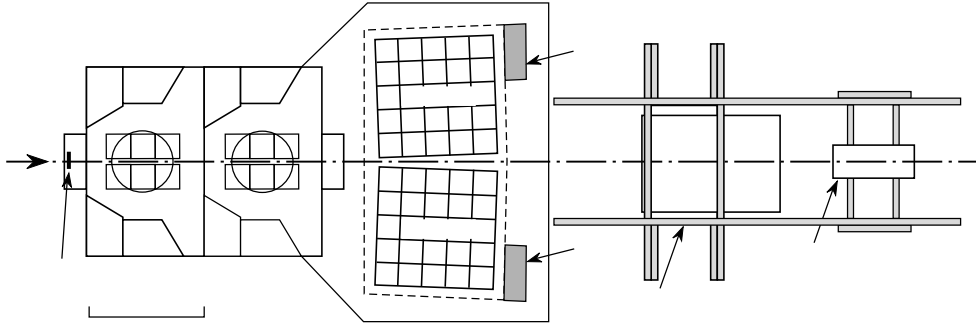


**Figure 1.** The NA49 experimental set-up.

**Table 1.** Acceptance of the various detectors.

| Detector | Particle                    | $y$       | $p_T$ (GeV) |
|----------|-----------------------------|-----------|-------------|
| VTPC     | $K_s^0$                     | 3.0–4.2   | 0.4–2.0     |
| MTPC     | $K_s^0$                     | 1.6–2.8   | 0.4–2.0     |
| TOF      | $K^+$ , $K^-$               | 2.5–3.3   | 0.0–1.5     |
| MTPC     | $K^+$ , $K^-$               | 2.65–3.65 | 0.0–1.5     |
| VTPC     | $\Lambda$ , $\bar{\Lambda}$ | 2.6–4.0   | 0.6–2.4     |
| MTPC     | $(\Lambda + \bar{\Lambda})$ | 1.8–2.2   | 0.6–2.0     |

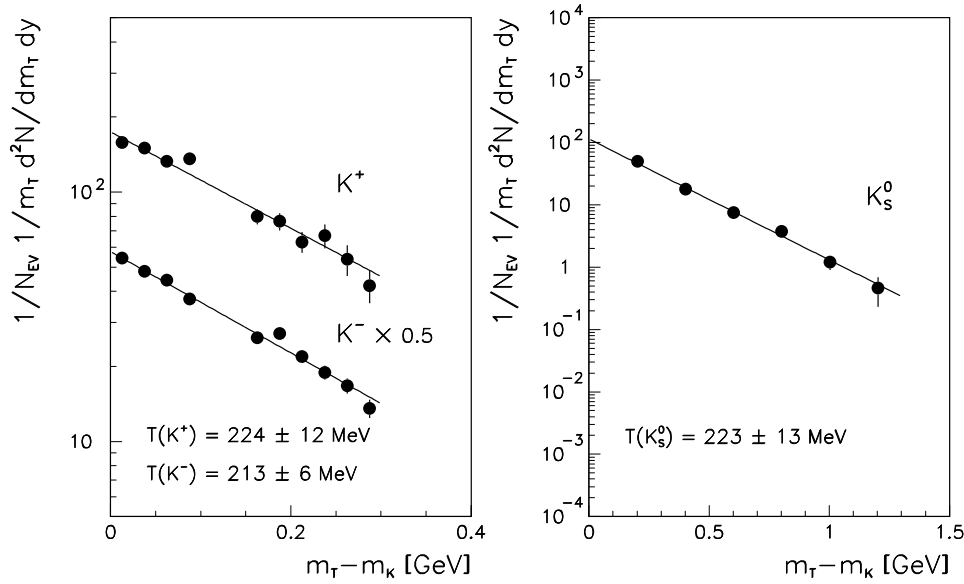
### 3.1. Neutral strange particles

Neutral strange particles are reconstructed via their charged decay products. The momentum of the decay tracks is obtained from the curvature of their trajectories in the VTPCs. After a geometrical fit of the position of the decay vertex and the momentum of the daughter tracks, the momentum of the neutral strange particles is calculated. Details about the analysis of  $\Lambda$ ,  $\bar{\Lambda}$  and  $K_s^0$  in the VTPCs can be found in [2].

In a special run neutral strange particles have also been measured in the MTPC with the target located directly in front of the MTPC. Because of the absence of a magnetic field, the momentum of the particles cannot be measured directly. It is calculated from the measured angles and from momentum and energy conservation. Due to the missing charge information of the decay particles,  $\Lambda$  can not be distinguished from  $\bar{\Lambda}$  in this special run.

### 3.2. Charged kaons

Charged kaons are identified by three different methods in the NA49 experiment. One method uses the decay topology of the kaon into a charged and a neutral particle for identification. The charged kaons are also identified by their specific energy loss in the MTPC or by their TOF. In the momentum range  $3 \leq p \leq 7 \text{ GeV } c^{-1}$  a combination of  $dE/dx$  and TOF methods is used.

Pb+Pb, NA49  $K^+$ ,  $K^-$ ,  $K_s^0$  Preliminary

**Figure 2.** The transverse mass spectra of  $K^+$  and  $K^-$  ( $2.5 < y < 3.3$ ) and  $K_s^0$  ( $2.0 < y < 2.7$ ) divided by the corresponding width of the rapidity intervals.

#### 4. Transverse mass distributions

The transverse mass is calculated from the transverse momentum as:

$$m_T = \sqrt{p_T^2 + m_0^2} \quad (1)$$

where  $m_0$  is the rest mass of the particle.

The transverse mass spectra are shown in figures 2 and 3. The shape of the distributions is approximately exponential over the full range.

The distribution is fitted with the function originating from thermal models

$$\frac{d^2n}{dm_T dy} = C m_T e^{-\frac{m_T}{T}} \quad (2)$$

with  $C$  and  $T$  as fit parameters. The inverse slope parameter ( $T$ ) is often referred to as ‘temperature’. The  $T$  parameter for the three kaon species is similar and is in the vicinity of 220 MeV. Both  $\Lambda$  and  $\bar{\Lambda}$  have a comparable slope parameter of about 280 MeV.

The dependence of the slope parameter  $T$  on the particle mass is shown in figure 4. All temperatures are obtained from the same data set. The slope parameters of particles with the same mass are averaged. In the case of the  $\Xi$  the temperature has only been determined for the sum of  $\Xi$  and  $\bar{\Xi}$  [3].

The slope parameter increases monotonically with the particle mass. This suggests the existence of a collective transverse flow. The data can be well described by a hydrodynamical model [4].

Figure 5 shows the inverse slope parameter as a function of the number of participant nucleons  $\langle N_P \rangle$  for  $\Lambda$  and for  $K_s^0$  produced in different collision systems ( $p + S$ ,  $S + S$ ,

Pb+Pb, NA49 Preliminary

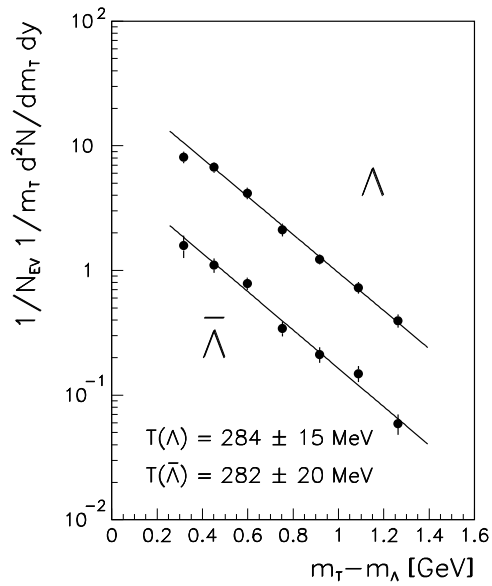


**Figure 3.** The transverse mass spectra of  $\Lambda$  and  $\bar{\Lambda}$  ( $2.6 < y < 3.8$ ). The spectra are divided by the width of the rapidity interval.

Pb+Pb, NA49 Preliminary

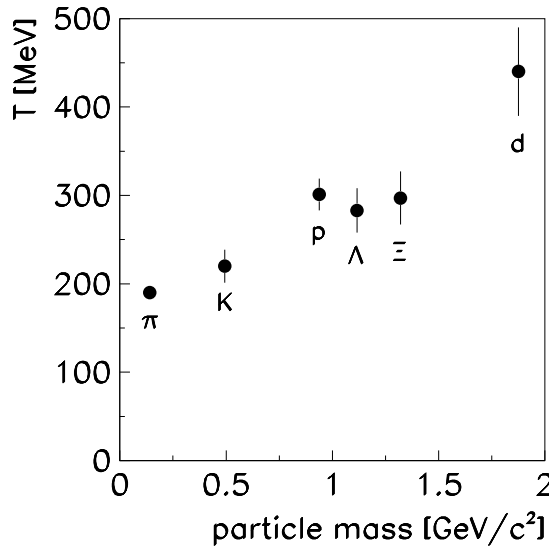


**Figure 4.** Inverse slope parameter of various particles produced in central Pb + Pb collisions at 158 GeV per nucleon.

S + Ag, S + Au [6], and Pb + Pb). A pronounced increase of the slope parameter with the system size is observed for  $\Lambda$ . The increase for  $K_s^0$ , if any, is significantly weaker.

### 5. Rapidity distributions

The rapidity density distribution is obtained by integrating the transverse mass spectra. The transverse mass distribution is extrapolated to regions outside of the NA49 acceptance by using the parametrization given in equation (2).

## Pb+Pb, NA49 Preliminary

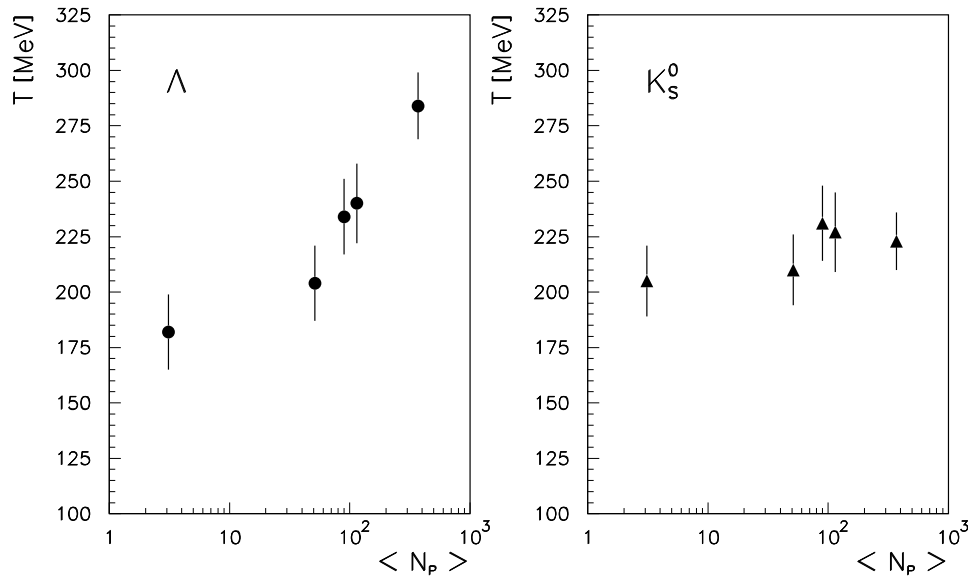


**Figure 5.** Inverse slope parameters of  $\Lambda$  (left) and  $K_s^0$  (right) for various target-projectile systems as a function of the number of participants.

In figure 6, the rapidity distributions for charged kaons (left) and  $K_s^0$  (right) are presented. Full symbols are measured values, open symbols have been reflected at mid-rapidity ( $y_K = 2.9$ ). The two independent measurements of the charged kaons in the MTPC and in the TOF walls agree within the errors. At mid-rapidity, a ratio  $K^+/K^- \approx 1.8$  is observed. This indicates a baryon rich region at mid-rapidity. The differences in the  $K_s^0$  measurements in MTPC and VTPC are an indication of the systematic uncertainty in the integrated yield. The systematic error is estimated to be about 20%. The  $K_s^0$  Pb + Pb data is overlaid with a scaled parametrization of the S + S rapidity distribution [6]. The scaling factor of 6.5 is about the ratio of the number of participants in the two systems.

Figure 7 shows the rapidity distribution for  $\Lambda$  (left) and  $\bar{\Lambda}$  (right). The Pb + Pb data is overlaid with the S + S rapidity distribution [6] and with a fit to the p + p data [7]. While the shape of the  $\bar{\Lambda}$  rapidity distribution does not change significantly, the  $\Lambda$  distribution exhibits a strong variation from the two-peak distribution in p + p over the flat distribution in S + S to a peak around mid-rapidity in Pb + Pb. The  $\Lambda$  (and  $\bar{\Lambda}$ ) yield includes a contribution of  $\Sigma^0$  which decay electromagnetically into  $\Lambda$  and cannot be distinguished from them experimentally. The yields also contain a fraction of the  $\Lambda$  (and  $\bar{\Lambda}$ ) from the decay of multi-strange particles which have not been removed by a cut on the impact parameter of the neutral strange particle at the main vertex. An investigation of the magnitude of this contribution is in progress.

The ratio  $\bar{\Lambda}/\Lambda \approx 0.2$  at mid-rapidity supports the hypothesis of a baryon rich region already inferred from the  $K^+/K^-$  ratio. This observation is consistent with the net proton rapidity distribution [5].

Pb+Pb, NA49 Preliminary

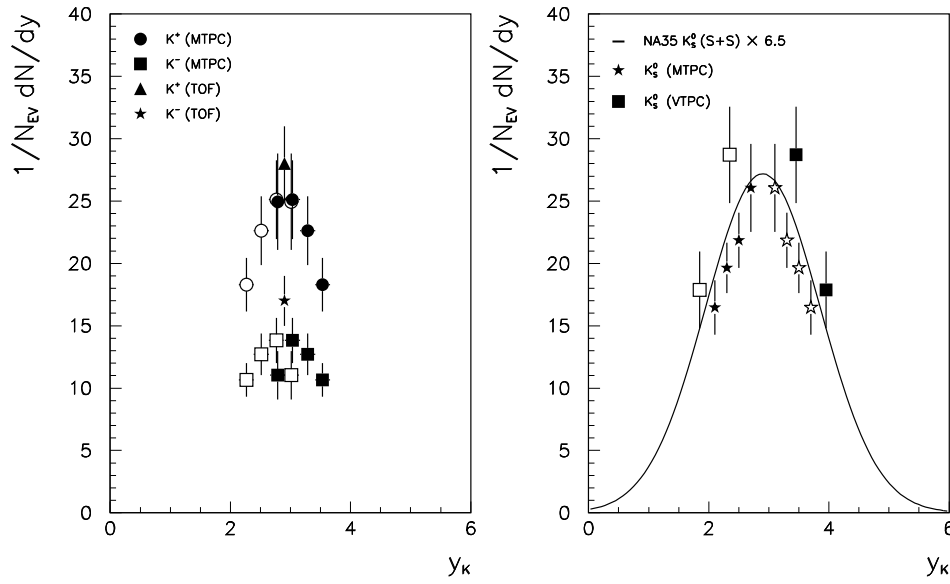


**Figure 6.** Rapidity distributions of  $K^+$  and  $K^-$  (left) and  $K_s^0$  (right) measured in the various NA49 detectors. The open symbols are the measured points reflected at mid-rapidity. The  $K_s^0$  distributions are overlaid with a scaled fit to the S + S data.

Pb+Pb, NA49 Preliminary

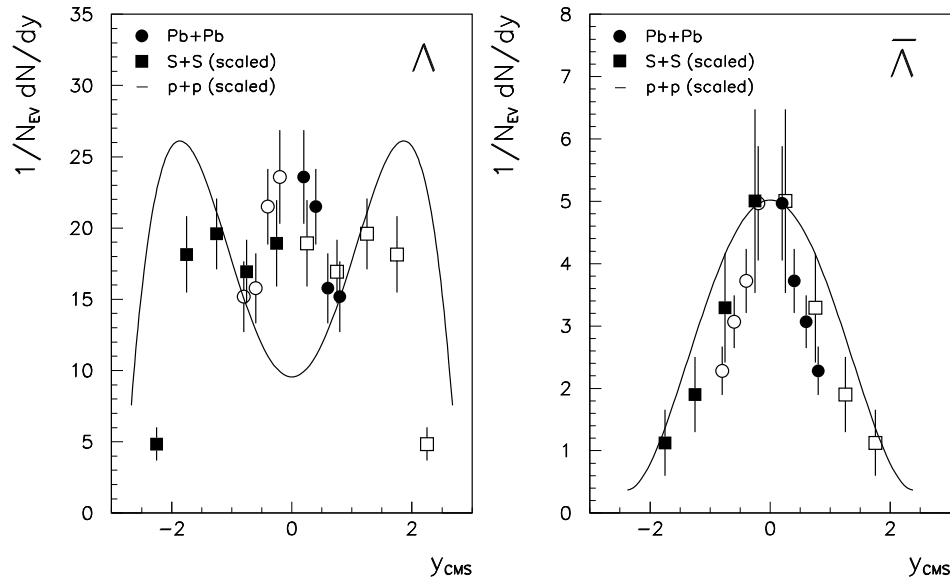


**Figure 7.** Rapidity distributions of  $\Lambda$  (left) and  $\bar{\Lambda}$  (right) produced in Pb + Pb, S + S, and p + p collisions at SPS energies. The open symbols are the measured points reflected at  $y_{CMS} = 0$ . The S + S data have been scaled by an arbitrary factor of 8.5 for  $\Lambda$  and 5.5 for  $\bar{\Lambda}$ . The lines represent fits to the scaled p + p data in order to compare the functional form.

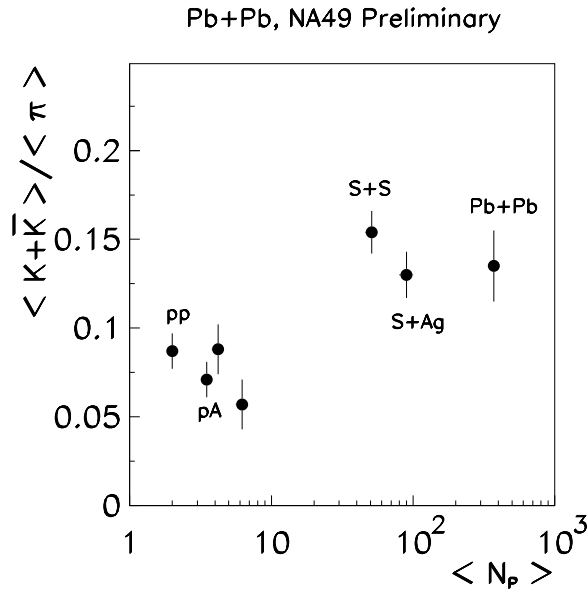


**Figure 8.** The dependence of the  $K/\pi$  ratio, defined as the sum of the multiplicities of all kaons ( $K^+$ ,  $K^-$ ,  $2K_s^0$ ) divided by all pions ( $\pi^+$ ,  $\pi^-$ ,  $\pi^0$ ), on the number of participant nucleons.

## 6. Kaon/pion ratio

The large acceptance for kaons allows the estimation of the kaon yields over full phase space. The extrapolation is performed by using the functional form of the S + S distribution which is in good agreement with the Pb + Pb data. The ratio  $\langle K + \bar{K} \rangle / \langle \pi \rangle$  is obtained by using the pion multiplicities measured in the same data sample [5]. This value is compared with S + S, S + Ag [6], N + N and p + A data [7] in figure 8. The p + A collision systems show no enhancement compared with proton–proton. There is a jump when going to the sulphur-nucleus systems with an enhancement of a factor of about two, but no further enhancement is observed in Pb + Pb collisions.

## 7. Summary

The NA49 experiment measures strange particles with a wide phase-space acceptance. The slope parameters of the transverse mass distributions increase with the particle mass and with the size of the collision system. The ratios  $K^+/K^- \approx 1.8$  and  $\bar{\Lambda}/\Lambda \approx 0.2$  indicate a baryon rich region at mid-rapidity. This is consistent with the net proton-rapidity distribution. A strong variation of the rapidity distribution of lambdas is observed with increasing system size. The shape of the distribution changes from two separated peaks in p + p collisions to a single peak centred at mid-rapidity in Pb + Pb collisions. A strangeness enhancement by a factor of  $\approx 2$  was seen in S + A collisions compared with N + N and p + A. There is no further enhancement in Pb + Pb.

## Acknowledgments

This work was supported by the Bundesministerium für Bildung und Forschung, Germany, the US Department of Energy under contract DE-AC03-76SFF00098, the Research Secretariat of the University of Athens, the Polish State Committee for Scientific Research



(under grant 2 P03B 101 10), the Polish–German Foundation, the Hungarian Scientific Research Foundation and the UK Engineering and Physical Science Research Council.

**References**

- [1] Koch P, Müller B and Rafelski J 1986 *Phys. Rep.* **142** 167
- [2] Yates T and the NA49 Collaboration 1997 *J. Phys. G: Nucl. Part. Phys.* **23** 1889
- [3] Odyniec G and the NA49 Collaboration 1997 *J. Phys. G: Nucl. Part. Phys.* **23** 1827
- [4] Kämpfer B 1997 *J. Phys. G: Nucl. Part. Phys.* **23** 2001  
Kämpfer B 1996 *Preprint* FZR-149, hep-ph/9612336
- [5] Afanasiev S V *et al* NA49 Collaboration 1996 *Nucl. Phys. A* **610** 188
- [6] Alber T *et al* NA35 Collaboration 1994 *Z. Phys. C* **64** 195
- [7] Gaździcki M and Hansen O 1991 *Nucl. Phys. A* **528** 754  
Białkowska H *et al* 1992 *Z. Phys. C* **55** 491